JOURNAL OF AIRCRAFT
Vol. 47, No. 2, March–April 2010

Engineering Notes

Experimental Studies on Transitional and Closed Cavity Configurations Including Flow Control

C. Lada*
Delft University of Technology, 2629 HS Delft, The Netherlands
and
K. Kontis†
University of Manchester, Manchester, England M60 1QD, United Kingdom

DOI: 10.2514/1.46027

Nomenclature

D = cavity depth, mm
L = cavity length, mm
M_∞ = freestream Mach number
X_c = distance from cavity leading edge, mm

I. Introduction

THERE are a wide range of aerodynamic problems due to the presence of cavities. Cavities can generate both steady and unsteady flow disturbances according to their geometry. Changes in mean static-pressure distributions inside the cavity can result in large pressure gradients, and the unsteady flow disturbances can generate self-sustaining oscillations which, in turn, generate acoustic tones that radiate from the cavity. Both the steady and the unsteady flows can present difficulties for store separation from an internal weapons bay. The steady flows can generate large nose-up pitching moments, and the unsteady flows can induce structural vibration. To ensure safe carriage and separation for transonic and supersonic speeds, a better understanding of the physics of cavity flows must be obtained.

The main variable affecting cavity flow is the length-to-depth ratio (L/D) and this is the reason that a very common way that cavity flows are classified in the literature is as open, transitional, and closed. The first cavity flowfield type identified for transonic and supersonic speeds generally occurs when the cavity is deep (a small value of L/D), as is typical of bomber aircraft bays, and is termed open cavity flow. Open flow occurs in cavities with values of L/D less than or equal to 10 for supersonic speeds and up to a maximum value between 6 and 8 for transonic speed. For this regime, the flow essentially bridges the cavity and a shear layer is formed over the cavity. At supersonic conditions, backflow within the cavity causes a weak shock wave at the leading edge to adapt the freestream flow to the high pressure over the mouth of the cavity. A shock wave is also generated at the rear edge to readapt the shear layer to the freestream flow [1]. This flow produces a nearly uniform static-pressure distribution along the floor of the cavity, which is desirable for safe store separation.

The second type of cavity flow identified for transonic and supersonic speeds occurs for cavities that are shallow (large values of L/D), as is typical of missile bays on fighter aircraft, and is termed closed cavity flow. Closed flow occurs in supersonic speeds for cavities with values of L/D greater than or equal to 13 and in transonic speeds for values down to a minimum between 9 and 15. In this regime, the flow separates at the forward face of the cavity, reattaches at some point along the cavity floor, and separates again before reaching the rear cavity face. At supersonic speeds the flow is further characterized by expansion waves at the front and rear of the cavity and floor impingement and exit shock waves emanating from within the cavity. This flow produces a mean static-pressure distribution with low pressure in the forward region, a plateau in the attached region, and high pressure in the aft region. Impingement and exit shocks are observed. The adverse static-pressure gradient produced by closed cavity flow can cause the separating store to experience large pitching moments that turn the store nose into the cavity. Acoustic tones generally do not occur for closed cavity flow [1].

The third and fourth cavity flowfield types defined for transonic and supersonic speeds are termed transitional (transitional-open and transitional-closed). These are flowfields that occur at supersonic speeds for cavities that have values of L/D that fall between closed and open cavity flow, that is, values of L/D between approximately 10 and 13 [1].

Little research has been performed on closed cavities and even less in transitional cavities. Firstly, they occur less often in the aircraft industry because of the size of weapons. Secondly, there are more complex types of flow structure and problems regarding open cavities because the flow is three dimensional. The interested reader in these complex flows is referred to several important publications [2–5]. Finally, the flow structure in cavities has in general been assumed as two dimensional. Therefore, the closed cavity flow can be assumed as the same as flow over a backward-facing step followed by flow over a forward-facing step. Historically, somebody could argue that research on cavities started as early as the late 19th century when resonance was first discovered by H. L. F. Helmholtz. Rayleigh [2] extended this work further, making corrections on energy relations for different mouth geometries. Further work on cavities was not continued until the late 1930s.

Johannesen [6] in 1954 investigated open and closed cavity flows. He used Schlieren photographs and pressure measurements and typified the open cavity flow by a series of weak compression waves above the shear layer. The intensity of the compression waves increased up to the critical aspect ratio. In the second classification, where the aspect ratio is greater than 13, the cavity is considered shallow and creation and rollup of vortices at the leading edge of the cavity takes place. Morozov [7] investigated the flow structure in a closed cavity in the compressible flowfield in 1958. He obtained experimental results on the distribution of the static pressure, recovery coefficients, and heat transfer. The dividing streamline was found to be similar to the incompressible flowfield. A closed-flow shock structure was characterized by an expansion fan at separation from the leading-edge corner with a shock wave at reattachment region to the base of the cavity. Another shock wave appeared at separation, when the trailing-edge step was approached and another expansion fan over the top of the trailing-edge step. He also defined that the length-to-depth ratio at which the flow structure changed from open to closed was between 13 and 14. Nowadays, the scientific society counts numerous studies that have been done on cavity flows at transonic and supersonic speeds that are investigating several issues, either theoretically or experimentally [8–11].

Received 17 June 2009; revision received 30 September 2009; accepted for publication 22 November 2009.

*Faculty of Aerospace Engineering.
†School of Mechanical, Aerospace, and Civil Engineering, Sackville Street. Associate Fellow AIAA.

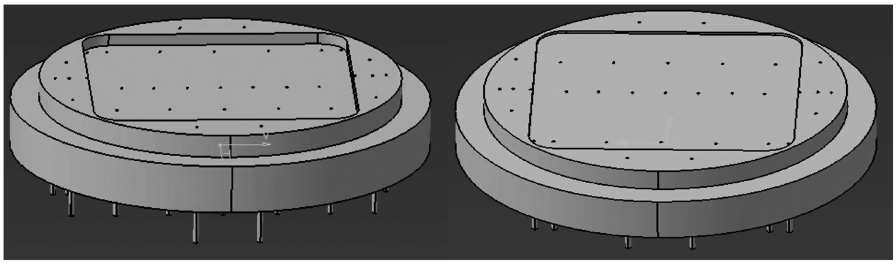

Fig. 1 Design of the cavity models ($L/D = 11$ and $L/D = 18$).

The main motivations of the present study are to provide further understanding of the flow physics of the steady phenomena inside transitional and closed cavities and also apply passive flow control to reduce or eliminate the undesired adverse pressure gradients observed in these flows. The passive flow control technique chosen in the current research work is sweeping the cavities' leading edge at different angles. This is expected to alter the position of the shear layer impingement inside the cavity to minimize the dynamic loads on the floor.

II. Experimental Setup

The experiments took place in the Plint TE25/A Supersonic wind tunnel. The wind tunnel is a high-speed closed-return facility, with a maximum Mach number of 1.7. The working area has a rectangular cross section of 100 mm in height, 26 mm in width, and 200 mm in length and a glass window allowing viewing of the test section during experiments. The pressure along the instrumented section is below atmospheric. The supersonic cavity models are four cubic models designed to fit to the access window of the tunnel with diameter 128 mm. The L/D ratios chosen to cover transitional and closed cavity flows are 11 and 18. The length of each is set to 90 mm. They are made of Perspex or aluminum. There are 33 static-pressure tappings; 17 of them are located inside the cavity and 16 outside the cavity on the circular plate. The pressure tappings inside the cavity are placed in three lines parallel to each other and to the direction of the flow. The middle line of tappings is located exactly in the center of the cavity. The upper line is located 24 mm up and the lower line 40 mm down with respect to the middle line. The pressure tappings were of 1 mm internal bore. Figure 1 shows the design of the cavities and Table 1 the location of the pressure tappings with (0,0) reference the center of the cavity.

Table 1 Coordinates of each pressure tapping

Pressure tapping number	x, mm	y, mm
1	−1.15	5.4
2	1.15	5.4
3	−5.4	2.4
4	−4	2.4
5	−2	2.4
6	0	2.4
7	2	2.4
8	4	2.4
9	5.4	2.4
10	−6	0
11	−5.4	0
12	−4.8	0
13	−3.6	0
14	−2.4	0
15	−1.2	0
16	0	0
17	1.2	0
18	2.4	0
19	3.6	0
20	4.8	0
21	5.4	0
22	6	0
23	−5.4	−1.7
24	5.4	−1.7
25	−4.7	−5
26	−3.9	−5
27	−2	−5
28	0	−5
29	2	−5
30	3.9	−5
31	4.7	−5
32	−1.15	−5.4
33	1.15	−5.4

Only the middle line set of pressure data is reported in this paper, because it contained more information than the rest.

Four different wedges were manufactured for each supersonic cavity model. The wedges were designed at four different angles of 15, 30, 45, and 60 deg and placed at the leading edge of the cavity. Figure 2 shows the design of the four different wedges.

This work considered only mean flow effects. Average pressures inside and around the cavities were obtained via the aid of SenSym part number ASDX015 pressure transducers with a range 0–15 psi. For each L/D the pressure readings were taken at freestream Mach number of 0.8, 1.4, and 1.7 and the Reynolds numbers were 6.25×10^5, 1.09×10^6, and 1.3×10^6, respectively (based on the freestream velocity and the chord length of the fin at the root). The pressure uncertainty in the transducer data was 2%. Oil flow technique was employed to visualize the surface flow inside and around the cavity, using a mixture of titanium dioxide with linseed oil and silicon. The experiments were repeated for each wedge, placed both at leading and trailing edge of each cavity, Fig. 2.

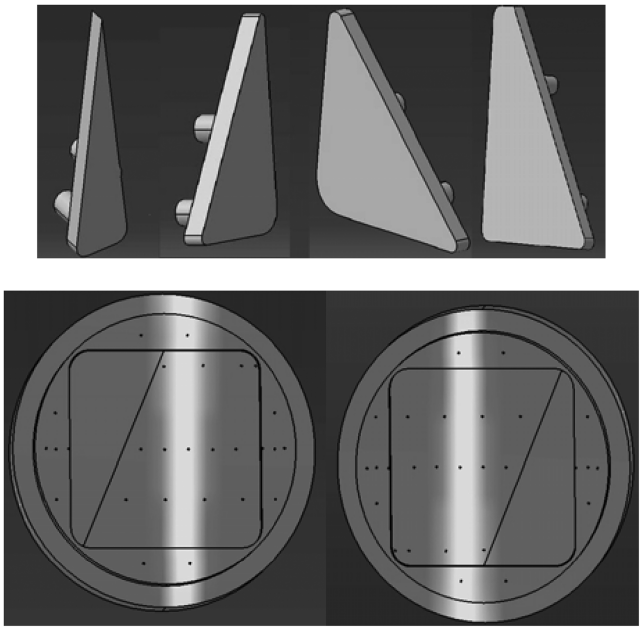

Fig. 2 Design of the four insert wedges (15, 30, 45, and 60 deg) and location of the 30 deg wedge at the leading and trailing edge of the cavity.

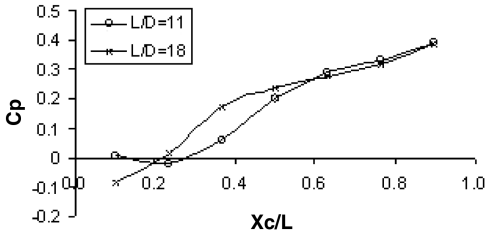

Fig. 3 Cavity flow pressure distribution for open cavities $L/D = 11$ and 18 at Mach 0.8.

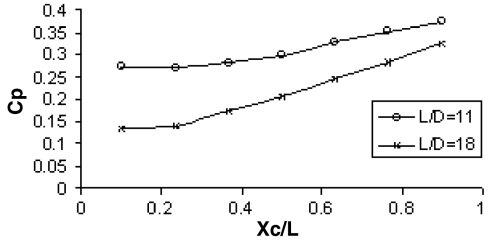

Fig. 4 Cavity flow pressure distribution for open cavities $L/D = 11$ and 18 at Mach 1.4.

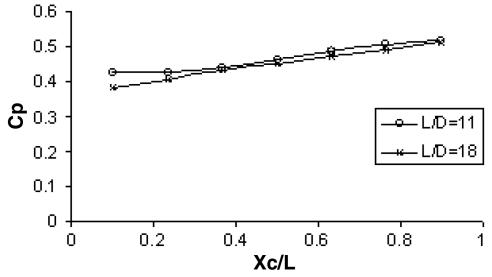

Fig. 5 Cavity flow pressure distribution for open cavities $L/D = 11$ and 18 at Mach 1.7.

III. Results and Discussion

A. Cavity Without Flow Control

1. Steady Pressure Measurements

For $L/D = 11$ and 18, Figs. 3–5 show the pressure coefficient distributions inside cavities for Mach numbers 0.8, 1.4, and 1.7, respectively. Figure 3 shows a typical transitional-closed cavity flow for $L/D = 11$, where the pressure coefficient is slightly negative in the first 20% of the length as the flow separates into the cavity and then the pressure steadily increases along the cavity floor to a maximum at the downstream end. The shear layer impingement point is located just before $Xc/L = 0.6$. Similar results were obtained for $L/D = 18$. This type of flow is transitional-closed, although a closed type of flow was expected for that aspect ratio (Fig. 3). For these two cases large longitudinal pressure gradients occur that can cause large pitching up moments. The pressure coefficient is negative in the first 20% and again steadily increases along the cavity floor.

As the Mach number increased to 1.4, the flow changed from transitional-closed to transitional-open for $L/D = 11$, Fig. 4. The pressure coefficient steadily increases along the cavity floor and there is no indication of shear layer impingement. The magnitude of pressure coefficient has increased, because the Mach number was increased. For $L/D = 18$, similar results were obtained.

At Mach number 1.7, no differences were recorded at the pressure distributions inside the two cavities, Fig. 5. Again, they both are transitional-open type. It appears that when the flowfield is transitional, increasing the Mach number causes the pressure distribution on the cavity floor to change in the direction of the open transitional flow. That effect was also observed by Stallings et al. [12].

2. Oil Flow Results

Figures 6–8 show the oil flow results for cavities $L/D = 11$ and 18 at Mach numbers 0.8, 1.4, and 1.7. The oil flow results are in good agreement with the pressure distributions. Figure 6 shows the location of the shear layer impingement for cavities $L/D = 11$ and $L/D = 18$ at $Xc/L = 0.6$ and $Xc/L = 0.4$, respectively. The flow before the shear layer impingement is a backflow and after the shear layer impingement is in the direction of the freestream. The flow separates just before the edges of each cavity.

Figure 7 shows that there is no shear layer impingement, which means that the cavity has changed from transitional-closed to

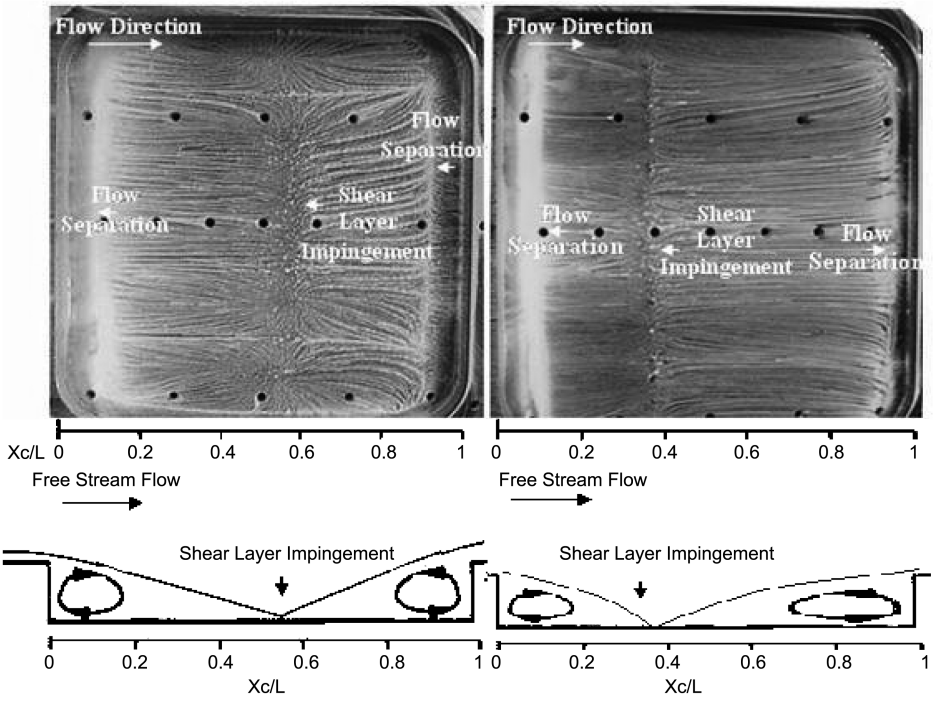

Fig. 6 Oil flow result for open cavity $L/D = 11$ and 18 at Mach 0.8 and schematic of flow structures within transitional cavity flow, side view.

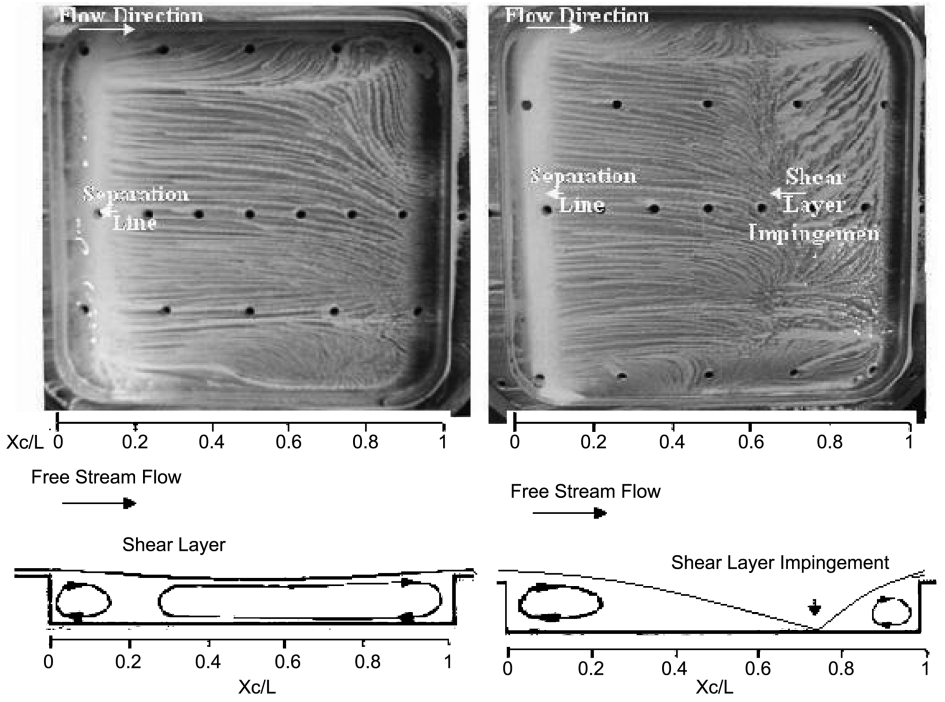

Fig. 7 Oil flow result for open cavity $L/D = 11$ and 18 at Mach 1.4 and schematic of flow structures within transitional cavity flow, side view.

transitional-open by increasing the Mach number. The same separation regions are observed as those at Mach number 0.8. For $L/D = 18$ the impingement point has moved closer to the trailing edge and is located now at $Xc/L = 0.65$; this is still a transitional-closed cavity even though the pressure distribution above indicated no signs of shear layer impingement.

When the Mach number was increased further no sign of shear layer impingement was observed on any of the two cases.

Evidences of three-dimensional effects close to the side walls of the cavity were first observed for $L/D = 11$ at Mach 1.4 where the separation lines did not appear straight any more nor symmetrical about the centerline. It was also found that the spanwise static-pressure distribution measured close to the wall was affected by the three-dimensional structures, but this will be discussed in a future publication.

B. Cavity with Flow Control

1. Steady Pressure Measurements

For $L/D = 11$ and 18, transitional cavity flowfield occurs. Because acoustic fields exist in transitional-open cavities and store-nose-up pitching moments exist in transitional-closed cavities, controlling the flow aims in suppressing the acoustic modes in transitional-open cavities as well as decreasing the longitudinal pressure gradients in transitional-closed cavities so that the problem of store-nose-up pitching moment is not severe. At $M = 0.8$ the cavity flowfield is transitional-closed for both cases. When the Mach number increased from 0.8 to 1.4 and finally to 1.7, the flowfield changed from transitional-closed to transitional-open.

For $L/D = 11$, Figs. 8–10, show the pressure coefficient distributions on the cavity floor with a 15 deg wedge placed at the forward and aft edge of the cavity at Mach numbers of 0.8, 1.4, and 1.7,

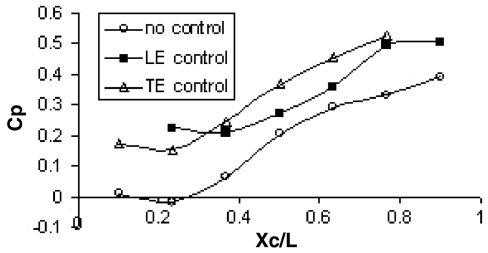

Fig. 8 Pressure distribution at Mach number 0.8 ($L/D = 11$ transitional cavity with 15 deg wedge on leading and trailing edge).

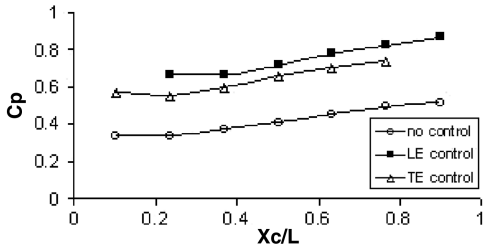

Fig. 10 Pressure distribution at Mach number 1.7 ($L/D = 11$ transitional cavity with 15 deg wedge on leading and trailing edge).

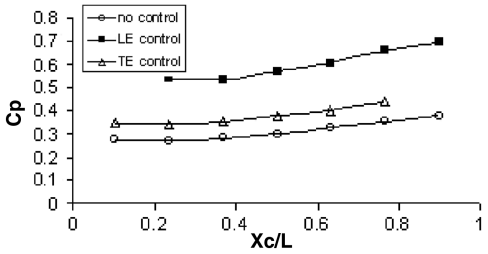

Fig. 9 Pressure distribution at Mach number 1.4 ($L/D = 11$ transitional cavity with 15 deg wedge on leading and trailing edge).

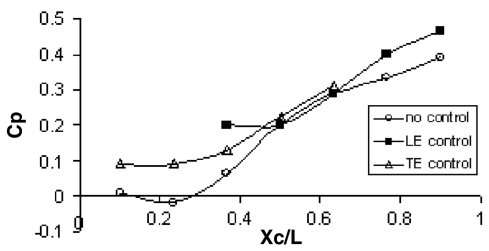

Fig. 11 Pressure distribution at Mach number 0.8 ($L/D = 11$ transitional cavity with 30 deg wedge on leading and trailing edge).

respectively. At $M = 0.8$ the cavity is transitional-closed type. Figure 8 shows an increase of pressure along the cavity floor, for both the leading- and trailing-edge cases. When the wedge was placed at the leading edge, a separation region was observed just aft of the leading edge as at the no control case and another separation region is indicated just before the cavity trailing edge, where a plateau is observed at $0.8 < Xc/L < 1$. The less severe adverse pressure gradient was observed when the wedge was placed at the leading edge. When the wedge was placed at the trailing edge the only effect on the flowfield was that the pressure was increased along the cavity floor, meaning that more flow was entrained in the cavity.

When the Mach number was increased to 1.4 and 1.7, the main flow features remained unaltered inside the cavity and the pressure in all cases has increased in magnitude, meaning that more flow was entrained.

For $L/D = 11$, Figs. 11–13, show the pressure coefficient distribution on cavity floor with a 30 deg wedge placed at the forward and aft edge of the cavity at Mach numbers of 0.8, 1.4, and 1.7, respectively. Figure 11 shows that the two control cases were almost equally effective for that case. When the 30 deg wedge was placed at the cavity leading edge, there was a dramatic increase of pressure at $Xc/L = 0.38$, which was followed by unaltered pressure distribution compared with the no control case until $Xc/L = 0.62$ and then there was a slight increase recorded close to the trailing edge. Compared with the no control case the longitudinal pressure gradient was decreased. When the 30 deg wedge was placed at the cavity trailing edge, again the pressure was increased at $0.1 < Xc/L < 0.38$ compared with the no control case and then at $0.38 < Xc/L < 0.62$, the pressure distribution was the same as for the other two cases. For that case, the longitudinal pressure gradient was reduced even more compared with the other two cases. When the Mach number increased to 1.4 and 1.7 the main flow features remained unaltered, and the pressure increased in magnitude apart from the case of the wedge placed at the trailing edge of the cavity at Mach number of 1.4 (Fig. 12), which remained at the same levels as the no control case.

For $L/D = 11$, Figs. 14–16, show the pressure coefficient distribution on the cavity floor with a 45 deg wedge placed at the forward and aft edge of the cavity at Mach numbers of 0.8, 1.4, and 1.7, respectively. Figure 14 shows that the leading-edge wedge has produced a concave up-shaped pressure distribution similar to an open cavity case. On the other hand, the same wedge placed at the trailing edge has dramatically increased the longitudinal pressure gradient causing more severe pitching moments inside the cavity. Similar flow behavior was obtained when the Mach number was increased to 1.7 (Fig. 16). At Mach number 1.4 the wedge placed at the leading edge increased the pressure inside the cavity and the wedge placed at the trailing edge reduced it.

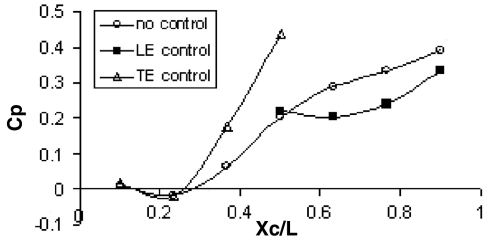

Fig. 14 Pressure distribution at Mach number 0.8 ($L/D = 11$ transitional cavity with 45 deg wedge on leading and trailing edge).

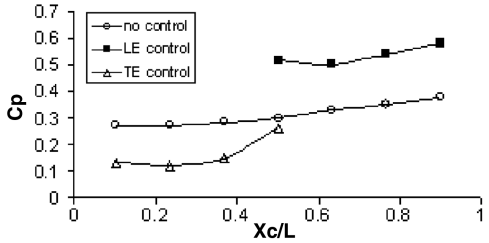

Fig. 15 Pressure distribution at Mach number 1.4 ($L/D = 11$ transitional cavity with 45 deg wedge on leading and trailing edge).

The 60 deg wedge covers more than half of the cavity storage volume and erroneous conclusions derived from the experimental results due to lack of pressure tappings.

For $L/D = 18$, Figs. 17–19, show the pressure coefficient distribution on the cavity floor with a 15 deg wedge placed at the forward and aft edge of the cavity at Mach numbers of 0.8, 1.4, and 1.7. The wedge placed at the leading edge of the cavity shows a separation region just after the leading edge of the cavity and also a movement of the shear layer impingement point from just before $Xc/L = 0.4$ to $Xc/L = 0.6$. The wedge also reduced the adverse pressure gradient compared with the no control case. When the wedge was placed at the trailing edge a favorable pressure gradient was observed. The flow separates around $Xc/L = 0.6$ just before its exits the cavity (Fig. 17). When the Mach number was increased to 1.4, similar results were obtained (Fig. 18). At Mach number 1.7, the wedge placed at the leading edge caused a dramatic pressure dropped

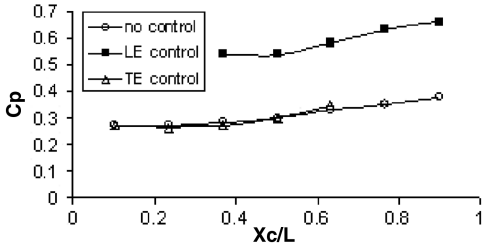

Fig. 12 Pressure distribution at Mach number 1.4 ($L/D = 11$ transitional cavity with 30 deg wedge on leading and trailing edge).

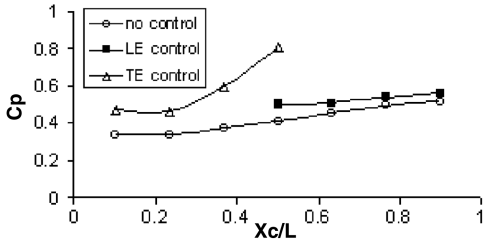

Fig. 16 Pressure distribution at Mach number 1.7 ($L/D = 11$ transitional cavity with 45 deg wedge on leading and trailing edge).

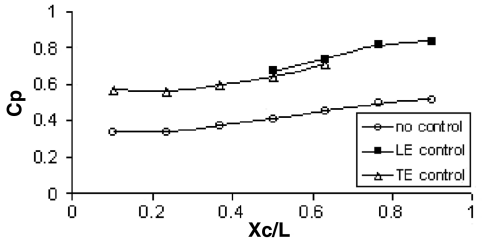

Fig. 13 Pressure distribution at Mach number 1.7 ($L/D = 11$ transitional cavity with 30 deg wedge on leading and trailing edge).

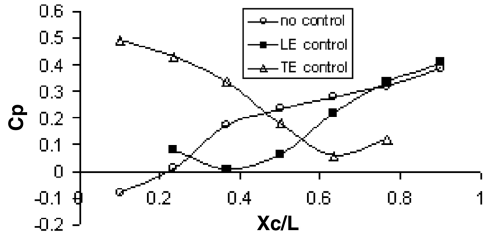

Fig. 17 Pressure distribution at Mach number 0.8 ($L/D = 18$ transitional cavity with 15 deg wedge on leading and trailing edge).

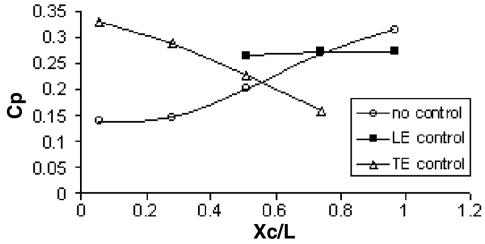

Fig. 18 Pressure distribution at Mach number 1.4 ($L/D = 18$ transitional cavity with 15 deg wedge on leading and trailing edge).

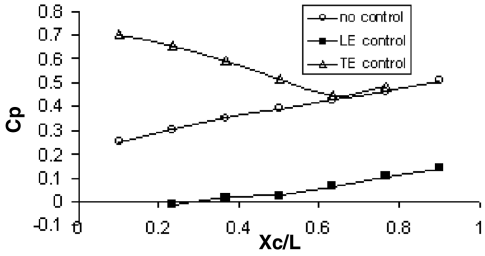

Fig. 19 Pressure distribution at Mach number 1.7 ($L/D = 18$ transitional cavity with 15 deg wedge on leading and trailing edge).

along the entire cavity floor and a very small adverse pressure gradient is observed. Again, the wedge at the trailing edge caused a favorable pressure gradient.

Figures 20–22 show the pressure coefficient distribution on the cavity floor with a 30 deg wedge placed at the forward and aft edge of the $L/D = 18$ cavity at Mach numbers of 0.8, 1.4, and 1.7, respectively. The wedge placed at the leading edge of the cavity causes a separation region just after the leading edge of the cavity and also a movement of the shear layer impingement point from just before $Xc/L = 0.4$ close to $Xc/L = 0.8$. The wedge also reduced the adverse pressure gradient compared with the no control case. When the wedge was placed at the trailing edge a favorable pressure gradient was observed (Fig. 20). When the Mach number was increased to 1.4, the wedge placed on the leading edge did not affect the pressure distribution compared with the no control case, and the wedge placed at the trailing edge caused a favorable pressure gradient (Fig. 21). At Mach number 1.7, the wedge placed at the leading edge caused a dramatic pressure dropped along the entire cavity floor and a very small adverse pressure gradient is observed.

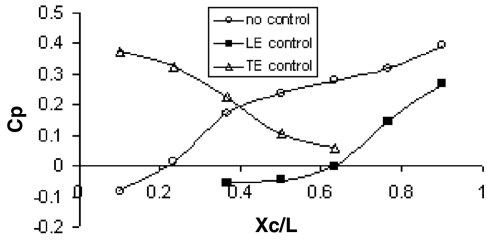

Fig. 20 Pressure distribution at Mach number 0.8 ($L/D = 18$ transitional cavity with 30 deg wedge on leading and trailing edge).

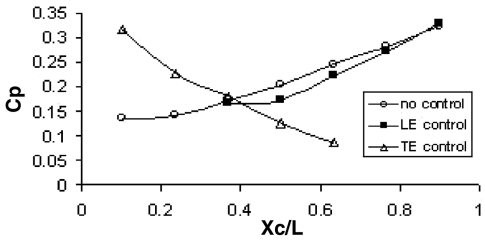

Fig. 21 Pressure distribution at Mach number 1.4 ($L/D = 18$ transitional cavity with 30 deg wedge on leading and trailing edge).

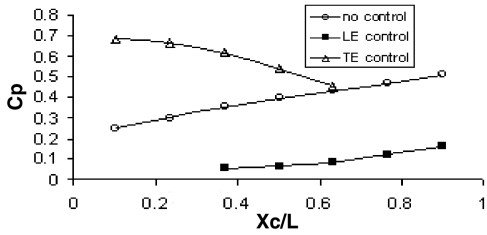

Fig. 22 Pressure distribution at Mach number 1.7 ($L/D = 18$ transitional cavity with 30 deg wedge on leading and trailing edge).

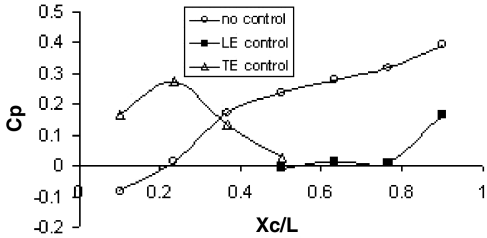

Fig. 23 Pressure distribution at Mach number 0.8 ($L/D = 18$ transitional cavity with 45 deg wedge on leading and trailing edge).

Again, the wedge at the trailing edge caused a favorable pressure gradient (Fig. 22).

Figures 23–25 show the pressure coefficient distribution on the cavity floor with a 45 deg wedge placed at the forward and aft edge of the $L/D = 18$ cavity at Mach numbers of 0.8, 1.4, and 1.7. The wedge placed at the leading edge of the cavity caused a dramatic decrease in pressure and also the adverse pressure gradient is reduced. When the wedge was placed at the trailing edge an adverse pressure gradient is observed until $Xc/L = 0.2$ and then the pressure starts dropping indicating signs of possible separation (Fig. 23). When the Mach number was increased to 1.4, the wedge placed on the leading edge did not affect the flow significantly, it only caused the pressure to decrease in magnitude. The wedge placed at the trailing edge shows a plateau region around $0.1 < Xc/L < 0.3$, which is possibly an impingement region, and then the pressure drops indicating possible separation (Fig. 24). At Mach number 1.7, similar results as the Mach number 1.4 case were obtained; the only difference is that by increasing the Mach number the shear layer for the trailing-edge control case seems to impinge closer to the leading

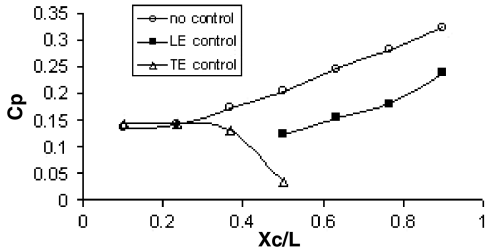

Fig. 24 Pressure distribution at Mach number 1.4 ($L/D = 18$ transitional cavity with 45 deg wedge on leading and trailing edge).

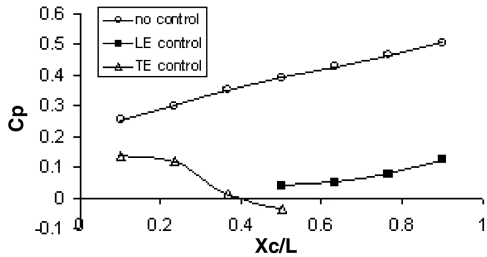

Fig. 25 Pressure distribution at Mach number 1.7 ($L/D = 18$ transitional cavity with 45 deg wedge on leading and trailing edge).

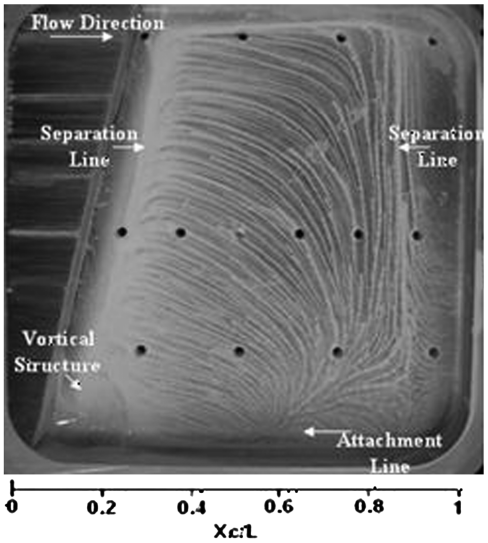

Fig. 26 Oil flow result for cavity $L/D = 11$, with 15 deg wedge placed at the leading edge, $M_\infty = 0.8$.

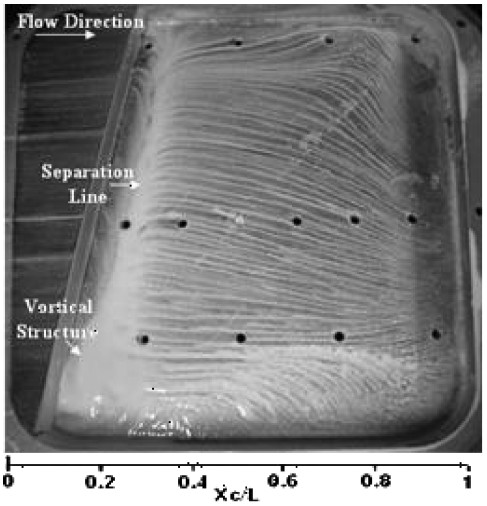

Fig. 27 Oil flow result for cavity $L/D = 11$, with 15 deg wedge placed at the leading edge, $M_\infty = 1.4$.

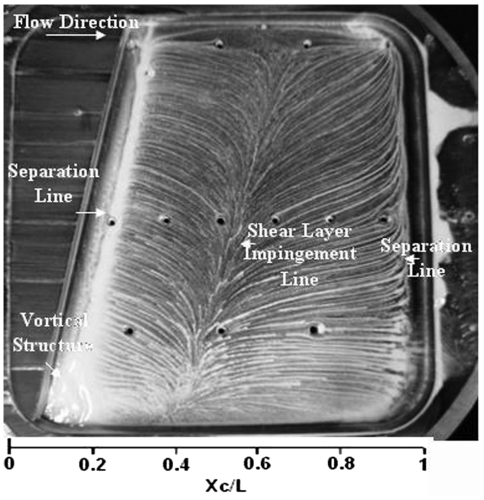

Fig. 28 Oil flow result for cavity $L/D = 18$, with 15 deg wedge placed at the leading edge, $M_\infty = 0.8$.

edge (Fig. 25). This effect of Mach number was also observed for the no control case.

The 60 deg wedge covers more than half of the cavity storage volume and erroneous conclusions derived from the experimental results due to lack of pressure tappings.

2. *Oil Flow Results*

Figures 26 and 27 show the oil flow results obtained when the 15 deg wedge was inserted in the $L/D = 11$ cavity at 0.8 and 1.4 Mach numbers, respectively. Figure 26, shows an attachment line just above the bottom edge of the cavity. It is possible that the sweep of the leading-edge wedge causes the shear layer impingement line to sweep as well. So part of the shear layer impinges inside the cavity where the attachment line is and part of it impinges somewhere on the rear edge of the cavity. As for the open cavity case, when the shear layer bridges the cavity part of it inflows and just forward of the trailing edge separates. Part of the flow moves upward and toward the aft edge of the cavity, which is a low-pressure region, and part of it moves downward and again toward the aft edge. Just before the leading edge the flow separates again and a line parallel to the sweep angle is observed. A tornado vortex is observed at the forward bottom side. The location of the separation lines are in good agreement with the pressure distribution (Fig. 8). Figure 27 show a similar flow pattern as the previous case but no separation line is observed close to the leading edge of the cavity; that also agrees with the pressure distribution for that case (Fig. 9). Unfortunately the flow patterns close to the bottom edge of the cavity became unclear as the wind tunnel was shut down. As the Mach number increased to 1.7, the same flow behavior was observed.

Similar flow behavior was observed for cavity $L/D = 11$ as the wedge angle increased.

Figure 28 shows the oil flow result of the cavity $L/D = 18$ when the 15 deg wedge was placed at the leading edge at Mach number 0.8. The pressure distribution for that case indicated a movement of the shear layer impingement point from just before $Xc/L = 0.4$ to $Xc/L = 0.6$ compared with the no control case (Fig. 17). Figure 28 is in good agreement with the pressure distribution data and shows that the shear layer impingement line is now parallel to the swept leading edge of the cavity. As always the separation line just ahead of the leading edge is observed, and a separation line just before the cavity trailing edge is also shown. When the Mach number increased to 1.4 and 1.7, similar results were obtained.

Similar flow behavior was observed for cavity $L/D = 18$ as the wedge angle increased.

IV. Conclusions

The study showed that transitional and closed cavity flows are highly dependent on the Mach number and the L/D ratio.

For the closed cavity case $L/D = 18$ the wedges placed at the leading edge reduced the adverse pressure gradient. The wedges placed at the trailing edge caused a favorable pressure gradient. These results were observed for all Mach numbers and all wedge angles. This is a very important observation for weapon release, because the reduction/elimination of the adverse pressure gradient reduces/eliminates the pitching up moments as well.

For the transitional cavity case $L/D = 11$, the wedges did not affect the flowfield as much as for the closed cavity case. By placing the wedges inside the transitional cavities the geometry changed such that the L/D ratio was reduced and the cavity's flowfield changed from transitional-closed to transitional-open and finally to open as the Mach number increased. Transitional-open and open cavities no longer hold characteristics of adverse pressure gradients.

References

[1] Tracy, B. M., and Plentovich, B. E., "Cavity Unsteady-Pressure Measurements at Subsonic and Transonic Speeds," NASA TP-3669, 1997.

[2] Roshko, A., "Some Measurements of Flow in a Rectangular Cutout," National Advisory Committee for Aeronautics TN-3488, 1955.

[3] Maull, D. J., and East, L. F., "Three-Dimensional Flow in Cavities," *Journal of Fluid Mechanics*, Vol. 16, No. 4, 1963, pp. 620–632. doi:10.1017/S0022112063001014

[4] Cattafesta, L. N., Williams, R. D., Rowley, W. C., and Farrukh, S. A., "Review of Active Control of Flow-Induced Cavity Resonance," AIAA Paper 2003-3567, 2003.

[5] Charwat, A. F., Roos, J. N., Dewey, C. F., and Hiltz, J. A., "An Investigation of Separated Flows—Part II Flow in the Cavity and Heat Transfer," *Journal of Aerospace Science*, Vol. 28, No. 6, 1961, pp. 457–470.

[6] Johannesen, N. H., "Experiments on Supersonic Flow Past Bodies of Revolution with Annular Gaps of Rectangular Section," *Philosophical Magazine*, Vol. 46, No. 372, 1955, pp. 31–39.

[7] Morozov, M. G., "Interaction between a Supersonic Stream and a Rectangular Depression on a Flat Plate," *Soviet Technical Physics Letters*, Vol. 3, No. 1, 1958, pp. 144–149.

[8] Plentovich, E. B., "Study of Three-Dimensional Cavity Flow at Transonic Speeds," AIAA Paper 88-2032, 1988.

[9] Wood, M. R., Wilcox, J. F., Bauer, X. S. S., and Allen, M. J., "Vortex Flows at Supersonic Speeds," NASA TP-211950, 2003.

[10] Zhang, X., Rona, A., and Edwards, A. J., "An Observation of Pressure Waves Around a Shallow Cavity," *Journal of Sound and Vibration*, No. 4, Vol. 214, 1998, pp. 771–778. doi:10.1006/jsvi.1998.1635

[11] Chung, K. M., "Characteristics of Transonic Rectangular Cavity Flows," *Journal of Aircraft*, No. 3, Vol. 37, 2000, pp. 463–468. doi:10.2514/2.2620

[12] Stallings, R. L., Plentovich, E. B., Tracy, M. B., and Hemsch, J. M., "Measurements of Store Forces and Moments and Cavity Pressures for a Generic Store in and Near a Box Cavity at Subsonic and Transonic Speeds," NASA Technical Memorandum 4611, 1995.